

Density-Functional Study of the Equilibrium Structures, Vibrational Spectra, and Energetics of CH₃OBr and CH₃BrO

Sujata Guha and Joseph S. Francisco

Department of Chemistry and Department of Earth and Atmospheric Sciences, Purdue University, West Lafayette, Indiana 47907-1393

Received: July 29, 1998; In Final Form: September 4, 1998

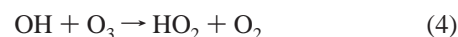
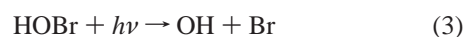
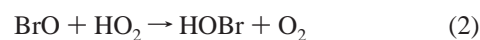
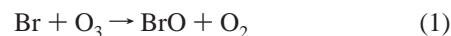
The geometries, vibrational spectra, and relative energetics of CH₃OBr and CH₃BrO have been examined using various ab initio and density-functional methods. The estimated heat of formation of CH₃OBr, at 0 K, is $-5.4 \text{ kcal mol}^{-1}$, in good agreement with the estimates of bond additivity. The CH₃BrO isomer is $42.6 \text{ kcal mol}^{-1}$ higher in energy than CH₃OBr.

I. Introduction

Bromine chemistry has been recognized, in recent years, to play a significant role in the stratospheric ozone budget¹ and in the Arctic troposphere during ozone-loss events.^{2,3} The discovery of massive seasonal depletion of ozone⁴ in the Antarctic spring centered attention on the role of biogenic and anthropogenic chlorinated species in the polar regions. Analogous to the interactions of the chlorine species implicated in ozone depletion are the stratospheric bromine species.⁵ The potential role of bromine species on ozone depletion in the marine boundary layer, at mid-latitudes, has also been suggested.⁶

Bromine is present in atmospheric aerosol particles, precipitation, seawater, and organisms in seawater. Other sources of bromine that can reach the stratosphere (i.e., those that are not removed from the troposphere by rainout, reaction with OH radicals, or photolysis) are methyl bromide (used as soil fumigant), trifluoromethyl bromide (used as fire-retardant and refrigerant), and tetrabromobisphenol-A (used as fire-retardant in circuit boards). The most abundant of these source gases is methyl bromide (CH₃Br), which is produced naturally, mainly due to oceanic biological processes. Once released into the atmosphere, the bromine species are effective not only in destroying ozone, but in also inhibiting ozone formation by sequestering oxygen atoms in the bromide forms.

The coupling of bromine oxides with HO_x species (such as OH and HO₂ radicals) to destroy ozone has been of particular importance. In different parts of the atmosphere, ozone is partially depleted through cycles involving the reaction of BrO and HO₂ radicals, which have been investigated in the laboratory by Poulet et al.,⁷ Larichev et al.,⁸ and Elrod et al.⁹ Such a process should increase the recycling of bromine radicals and could be efficient in regions where the OH concentration profiles are significant. The first step in this catalytic cycle is the reaction of bromine atoms with ozone. The cycle is represented by the following scheme of reactions:



HOBr, produced during this reaction, is rapidly recycled into active bromine species through photodissociation in the stratosphere. It has been suggested that in the marine boundary layer, HOBr could be converted into active bromine species on an aerosol surface and that HOBr would also be converted into photochemically labile BrCl and Br₂ species on sulfuric acid, sea salt, or ice particles.^{6,10}

It has been postulated that, similar to the BrO + HO₂ reaction, the BrO + CH₃O₂ reaction is also important and may play a role in the ozone depletion cycle in the stratosphere and in the marine boundary layer at different latitudes.¹¹ In case of the BrO + CH₃O₂ reaction, the BrO gets converted to HOBr via



There can be another possible reaction channel in which BrO gets converted into bromine atoms via the reaction



The photolysis of HOBr, or the reaction of Br atoms with ozone, could lead to rapid ozone depletion. Reaction 7 may be oversimplified and may yield CH₃OBr via



TABLE 1: Computed Equilibrium Geometries (Å and deg) for CH₃OBr and CH₃BrO

species	coordinates	6-311++G(3df,3pd)			6-311++G(3d2f,3pd)		
		B3LYP	B3PW86	B3PW91	B3LYP	B3PW86	B3PW91
CH ₃ OBr	CO	1.423	1.414	1.416	1.424	1.415	1.417
	BrO	1.848	1.830	1.833	1.848	1.829	1.834
	CH	1.091	1.091	1.092	1.091	1.091	1.092
	CH'	1.091	1.092	1.093	1.091	1.092	1.093
	COBr	112.5	112.0	112.1	112.4	111.9	112.0
	HCO	104.0	104.2	104.2	104.0	104.3	104.3
	H'CO	111.8	111.9	111.9	111.8	111.8	111.9
	H'COBr	180.0	180.0	180.0	180.0	180.0	180.0
	CH ₃ BrO	CBr	1.974	1.950	1.953	1.975	1.951
BrO		1.712	1.694	1.697	1.711	1.693	1.696
CH		1.087	1.087	1.088	1.086	1.087	1.087
CH'		1.084	1.084	1.085	1.084	1.084	1.085
CBro		104.4	104.5	104.7	104.5	104.6	104.7
HCBBr		106.6	106.8	106.6	106.6	106.7	106.6
H'CBBr		106.1	106.4	106.5	106.1	106.5	106.5
H'CBro		180.0	180.0	180.0	180.0	180.0	180.0

It has been determined that oxybromides absorb light at longer wavelengths than the corresponding bromides, and therefore, the photolysis of the BrO species, and their participation in chain reactions, will contribute to ozone consumption. Benter et al.¹² reported the gas-phase UV-vis absorption spectrum of CH₃OBr in the wavelength range 230 < λ < 400 nm and compared their data with the available data from recent literature.¹³ The heat of the BrO + CH₃O₂ reaction process is unknown because the heat of formation of CH₃OBr has not been determined. However, Helleis et al.¹⁴ found evidence for the formation of CH₃OCl from the analogous ClO + CH₃O₂ reaction.

Aranda et al.¹¹ used the discharge flow-mass spectrometric method (DF-MS) with laser-induced fluorescence (LIF) to study the kinetics of the BrO + CH₃O₂ reaction at 298 K and obtained a rate constant of $(5.7 \pm 0.6) \times 10^{-12} \text{ cm}^3 \text{ molecule}^{-1} \text{ s}^{-1}$. It was found that the BrO + CH₃O₂ reaction is likely to be negligible in the stratosphere but is potentially significant in the marine boundary layer and can affect the flora and fauna of that region. The reaction may also significantly contribute to the ozone loss observed in the Arctic troposphere during spring.

There have been no ab initio molecular orbital studies conducted on CH₃OBr thus far. It is important to consider the possible existence of such an intermediate (and its isomeric forms) in order to evaluate its stability. Knowledge of the heat of formation of CH₃OBr is required in order to understand and assess its potential role in stratospheric chemistry. There are two plausible connectivities for CH₃OBr isomers, namely CH₃OBr and CH₃BrO. In the present work, we examine the structures, vibrational spectra, and relative energetics of CH₃OBr and CH₃BrO to gain sufficient knowledge about the participation of the isomers in the BrO + CH₃O₂ reaction scheme.

II. Computational Methods

Ab initio molecular orbital calculations are performed using the GAUSSIAN 94 program.¹⁵ All equilibrium geometries are fully optimized to better than 0.001 Å for bond distances and 0.1° for bond angles, with an SCF convergence of at least 10⁻⁹ on the density matrix and a root-mean-square (rms) force of 10⁻⁴ atomic units. The equilibrium geometries are optimized at various levels of theory using Schlegel's analytical gradient method, first with the B3LYP (Becke's nonlocal three-parameter exchange with the Lee-Yang-Parr correlation functional) method¹⁶ and then with the B3PW86 (Becke's three-parameter functional with the nonlocal correlation provided by the Perdew 86 expression)¹⁷ and B3PW91¹⁸ density functional methods, incorporating the effects of the large 6-311++G(3df,3pd) and

6-311++G(3d2f,3pd) basis sets. The harmonic vibrational frequencies and intensities of all species are calculated at the B3LYP, B3PW86, and B3PW91 levels of theory in conjunction with the 6-311++G(3df,3pd) and 6-311++G(3d2f,3pd) basis sets, using the geometries calculated at the B3LYP, B3PW86, and B3PW91 levels of theory with each of the basis sets. For estimating the vertical energies of low-lying excited electronic states, the configuration interaction singles method (CIS)¹⁹ is used with the 6-311++G(3df,3pd) and 6-311++G(3d2f,3pd) basis sets, using the geometries obtained at the B3LYP, B3PW86, and B3PW91 levels of theory. To improve the energies, single-point calculations are performed with the CCSD(T) (singles and doubles coupled-cluster theory including a perturbational estimate of the effects of connected triple excitations)²⁰ wave functions, using the 6-311++G(3df,3pd) basis set. The heat of formation of CH₃OBr is determined using an isodesmic reaction scheme and compared to its heat of formation computed at the CCSD(T) level of theory.

III. Results and Discussion

A. Equilibrium Structures and Vibrational Frequencies of CH₃OBr and CH₃BrO. To determine the structures and stability of CH₃OBr and CH₃BrO, computations were performed at the various levels of theory (B3LYP, B3PW86, and B3PW91) using the 6-311++G(3df,3pd) and 6-311++G(3d2f,3pd) basis sets. The optimized structural parameters of the isomers are provided in Table 1.

From computations, CH₃OBr appears to possess a staggered structure with C_s symmetry. At the B3LYP/6-311++G(3df,3pd) level of theory, the COBr angle is predicted to be 112.5°, formed primarily due to the strong repulsion between the lone pairs of electrons residing on the bromine and oxygen atoms. The large Br-O bond length in CH₃OBr (1.848 Å) can be attributed to the poor overlap between the 3d orbitals of the large bromine atom and the 2p orbitals of the comparatively smaller oxygen atom. Our calculated value of the Br-O bond length agrees very well with the Br-O bond length in HOBr (1.853 Å) computed by Lee at the CCSD(T)/TZ2P level of theory.²¹ The C-O bond length for CH₃OBr, at the B3LYP/6-311++G(3df,3pd) level of theory, is 1.423 Å. Microwave studies have been performed by Venkateswarha and Gordy,²² which show the C-O bond length in methanol (CH₃OH) to be 1.427 ± 0.007 Å. Thus, our calculations suggest that the C-O bond lengths in CH₃OBr and methanol are quite similar, the difference being only ca. 0.003 Å.

The other isomeric form is CH₃BrO, where the hypervalent

TABLE 2: Vibrational Frequencies (cm⁻¹) and Intensities (km mol⁻¹) for CH₃OBr and CH₃BrO

species	mode no.	mode symmetry	description	6-311++G(3df,3pd)						6-311++G(3d2f,3pd)						
				B3LYP		B3PW86		B3PW91		B3LYP		B3PW86		B3PW91		
				freq	int	freq	int	freq	int	freq	int	freq	int	freq	int	
CH ₃ OBr	1	a'	CH ₃ asym str	3099	8	3118	7	3112	8	3100	8	3118	7	3112	8	
	2		CH ₃ sym str	3012	39	3021	39	3016	40	3012	39	3021	39	3016	40	
	3		CH ₃ asym dfm	1506	13	1500	13	1499	13	1506	13	1500	13	1499	13	
	4		CH ₃ sym dfm	1457	4	1451	3	1450	3	1456	4	1450	3	1450	3	
	5		CH ₃ rock	1188	18	1190	21	1189	20	1187	18	1189	21	1188	20	
	6		CO str	1010	47	1040	45	1035	45	1009	47	1038	45	1034	45	
	7	OBr str	595	6	615	7	612	7	592	6	613	7	609	7		
	8	COBr bend	316	2	318	2	317	2	316	2	318	2	316	2		
	9	a''	CH ₃ asym dfm	3082	29	3097	27	3092	28	3083	28	3097	26	3092	27	
	10		CH ₃ asym dfm	1463	9	1456	10	1456	10	1463	9	1456	10	1456	10	
	11		CH ₃ rock	1170	1	1170	1	1169	1	1170	1	1170	1	1168	1	
	12		torsion	234	3	236	3	235	3	234	3	237	3	235	3	
CH ₃ BrO	1		a'	CH ₃ asym str	3181	0	3194	0	3189	0	3182	0	3195	0	3189	0
	2			CH ₃ sym str	3066	4	3075	3	3070	3	3067	4	3075	3	3070	3
	3	CH ₃ asym dfm		1465	8	1458	9	1457	9	1464	8	1457	9	1456	9	
	4	CH ₃ sym dfm		1296	5	1293	3	1293	3	1295	5	1292	3	1291	3	
	5	CH ₃ rock		932	3	932	3	932	3	931	3	931	3	930	3	
	6	BrO str		723	39	765	42	759	42	720	39	761	42	755	42	
	7	CBr str	530	2	557	2	554	2	529	2	556	2	553	2		
	8	CBrO bend	222	6	227	6	227	6	221	6	225	6	226	6		
	9	a''	CH ₃ asym str	3197	0	3210	0	3205	7	3199	0	3211	0	3206	0	
	10		CH ₃ asym dfm	1441	9	1432	10	1431	10	1439	9	1431	10	1430	9	
	11		CH ₃ rock	938	2	939	2	938	2	936	2	938	2	937	2	
	12		torsion	128	0	130	0	131	0	130	0	132	0	132	0	

bromine atom lies in place of the oxygen atom of CH₃OBr. The structure of CH₃BrO also appears to possess C_s symmetry. For CH₃BrO, it is important to note that the lone pairs of electrons on the terminal oxygen atom sometimes tend to enter into resonance with the bonding electron pair of the Br–O bond, in which process the Br–O bond attains a partial double-bond character. This resonance effect is not observed with the oxygen atom that is sandwiched between the carbon and bromine atoms in CH₃OBr. Due to this partial double-bond character in CH₃BrO, the repulsion between the lone pairs of electrons on bromine and oxygen atoms is partially offset by the repulsion between the lone electron pairs and the C–Br and Br–O bond pairs. Thus, the CBrO angle gets shrunk (104.4°) and is a little smaller than the HCBro angle (106.6°), which is primarily formed due to the repulsion between the H–C and C–Br bonds (with the added repelling input of the lone electrons on bromine). The partial double-bond character in CH₃BrO manifests its effect on the BrO bond length, which has a smaller value at the B3LYP/6-311++G(3df,3pd) level of theory (1.712 Å), compared to the BrO bond length value in CH₃OBr at the same level of theory. Our computed value of the Br–O bond length in CH₃BrO is comparable to the Br–O bond length in HBrO (1.731 Å), FBrO (1.661 Å), and BrBrO (1.690 Å) computed by Lee at the CCSD(T)/TZ2P level of theory.²¹

The calculated vibrational frequencies and intensities for CH₃OBr and CH₃BrO are provided in Table 2. For CH₃OBr, the most intense bands are the CH₃ symmetric stretch and CO stretch while the least intense bands are the COBr bend and CH₃ rock. The OBr stretch occurs at a lower frequency than the CO stretch, consistent with the larger O–Br bond length than that of the C–O bond. The OBr stretch in CH₃OBr agrees well with the OBr stretches in HOBr²³ and Br₂O.²¹ This information should be useful in the assignment of the experimental spectra of CH₃OBr. The vibrational frequencies of CH₃OBr also exhibit certain spectral features (CH₃ asymmetric and symmetric stretches and CO stretch) similar to CH₃OH.^{24,25}

For CH₃BrO, there is maximum absorption at 723 cm⁻¹. This is the BrO stretch, and it lies between the BrO stretches in HBrO and BrBrO.²¹ There appears to be very little absorption at 530

and 938 cm⁻¹ and extremely little or no absorption at 3181, 3197, and 128 cm⁻¹. The BrO stretch band of CH₃BrO would allow its clear distinction from CH₃OBr.

B. Excited States of CH₃OBr and CH₃BrO. A spectroscopic property that is particularly useful and important in the characterization of the electronic spectra of CH₃OBr and CH₃BrO is their vertical excitation energies. Configuration interaction with all singlet excited determinations, CIS, has been shown to be an effective method of surveying the excited states of closed-shell molecules with reasonable experience for polyatomic molecules.¹⁹ However, we note that the CIS results are, at best, qualitative, but nevertheless, they provide an avenue for identifying the most distinguishing features among the isomeric forms. The CIS vertical excitation energies and oscillator strengths (F) for CH₃OBr and CH₃BrO, calculated at the B3LYP, B3PW86, and B3PW91 levels of theory, are provided in Table 3 and compared to those of HOBr. Benter et al.¹² reported the UV–vis absorption spectra for CH₃OBr and HOBr, and they are included in Table 3.

Critical examination of the predicted electronic spectra of CH₃OBr and CH₃BrO reveals that there are certain features that would allow these two molecules to be distinctly characterized. For CH₃OBr, the excited states located at 8.1 and 8.2 eV have the most relative oscillator strengths while the excited state located at 4.0 eV has the least relative oscillator strength (0.0003) and consequently should be quite weak. In comparison, for HOBr, the excited state located at 7.6 eV has the maximum relative oscillator strength (0.0065) while the excited state located at 4.1 eV has the least relative oscillator strength (0.0001).

Experiments conducted¹² exploring the CH₃OBr spectrum reveal an excited state (¹A'') located at 3.6 eV, which is comparable to the ¹A'' excited state according to our calculation at the B3LYP/6-311++G(3df,3pd) level of theory located at 4.0 eV. Another excited state (¹A') that was distinctly revealed by the experiments¹² appeared to be located at 4.4 eV, comparable to our computed excited state at 4.9 eV. Thus, our calculations of the excited states of CH₃OBr agree well with experimental observation. In case of HOBr, experiments¹² were

TABLE 3: Calculated Vertical Excitation Energies and Oscillator Strengths for HOBr, CH₃OBr, and CH₃BrO

species	states	CIS/6-311++G(3df,3pd)//						CIS/6-311++G(3d2f,3pd)//						expt ^a
		B3LYP		B3PW86		B3PW91		B3LYP		B3PW86		B3PW91		
		ΔE (ev)	F (rel)	ΔE (ev)	F (rel)	ΔE (ev)	F (rel)	ΔE (ev)	F (rel)	ΔE (ev)	F (rel)	ΔE (ev)	F (rel)	
HOBr	¹ A''	4.1	0.0001	4.2	0.0001	4.2	0.0001	4.1	0.0001	4.2	0.0001	4.2	0.0001	3.66
	¹ A'	4.9	0.0034	5.0	0.0034	5.0	0.0034	4.9	0.0034	5.0	0.0034	5.0	0.0034	4.69
	¹ A''	7.6	0.0065	7.8	0.0199	7.8	0.0135	7.6	0.0067	7.9	0.0223	7.8	0.0145	
CH ₃ OBr	¹ A''	4.0	0.0003	4.2	0.0004	4.1	0.0004	4.1	0.0003	4.2	0.0004	4.1	0.0004	3.6
	¹ A'	4.9	0.0033	5.0	0.0033	5.0	0.0033	4.9	0.0033	5.0	0.0033	5.0	0.0033	4.4
	¹ A''	7.0	0.0014	7.2	0.0015	7.1	0.0014	7.0	0.0015	7.2	0.0015	7.1	0.0015	
	¹ A'	8.1	0.2981	8.2	0.1187	8.2	0.1187	8.1	0.2981	8.2	0.1181	8.2	0.1181	
	¹ A''	8.2	0.1184	8.3	0.2936	8.2	0.2947	8.2	0.1178	8.3	0.2934	8.3	0.2946	
	¹ A'	8.6	0.1015	8.6	0.1008	8.6	0.1009	8.6	0.1008	8.6	0.1000	8.6	0.1002	
CH ₃ BrO	¹ A''	4.1	0.0006	4.3	0.0005	4.2	0.0005	4.1	0.0006	4.3	0.0005	4.3	0.0005	
	¹ A'	4.9	0.0057	5.2	0.0062	5.1	0.0063	4.9	0.0057	5.2	0.0063	5.1	0.0063	
	¹ A''	6.2	0.0001	6.3	0.0001	6.3	0.0001	6.2	0.0001	6.3	0.0001	6.3	0.0001	
	¹ A''	7.3	0.0146	7.2	0.0147	7.3	0.0146	7.3	0.0146	7.2	0.0147	7.2	0.0146	
	¹ A'	8.1	0.1887	8.2	0.1808	8.1	0.1812	8.1	0.1893	8.2	0.1808	8.1	0.1819	
	¹ A'	8.4	0.0412	8.3	0.0402	8.3	0.0393	8.4	0.0409	8.3	0.0400	8.3	0.0391	

^a Benter, T.; Feldman, C.; Kirchner, U.; Schmidt, M.; Schmidt, S.; Schindler, R. N. *Ber. Bunsenges. Phys. Chem.* **1995**, *99*, 1144.

TABLE 4: Total Energies (hartrees) of Species in the Isodesmic Scheme

species	6-311++G(3df,3pd)				6-311++G(3d2f,3pd)		
	B3LYP	B3PW86	B3PW91	CCSD(T)	B3LYP	B3PW86	B3PW91
H ₂ O	-76.46451	-76.64039	-76.43416	-76.33743	-76.46446	-76.64034	-76.43411
HOBr	-2649.95629	-2650.92147	-2649.90784	-2648.23807	-2649.95659	-2650.92174	-2649.90810
CH ₃ OH	-115.77432	-116.09436	-115.72763	-115.55497	-115.77423	-116.09429	-115.72757
CH ₃ OBr	-2689.27248	-2690.38192	-2689.20744	-2687.46387	-2689.27254	-2690.38198	-2689.20750
CH ₃ BrO	-2689.20360	-2690.31464	-2689.14084	-2687.39377	-2689.20401	-2690.31508	-2689.14129

TABLE 5: Heats of Formation (kcal mol⁻¹) for CH₃OBr

levels of theory	isodesmic reaction	
	CH ₃ OBr + HOH → CH ₃ OH + HOBr	
	$\Delta H_{r,0}^\circ$	$\Delta H_{f,0}^\circ$
B3LYP/6-311++G(3df,3pd)	4.8	-4.2
B3PW86/6-311++G(3df,3pd)	4.9	-4.3
B3PW91/6-311++G(3df,3pd)	4.6	-4.0
B3LYP/6-311++G(3d2f,3pd)	4.7	-4.1
B3PW86/6-311++G(3d2f,3pd)	4.7	-4.1
B3PW91/6-311++G(3d2f,3pd)	4.5	-3.9
CCSD(T)/6-311++G(3df,3pd)	6.0	-5.4

able to distinctly identify excited states at 3.66 (¹A'') and 4.69 eV (¹A') compared to our computed excited states at 4.1 and 4.9 eV, respectively. For CH₃BrO, our calculations indicate that, similar to the spectrum of CH₃OBr, the excited state located at 8.1 eV possesses the maximum relative oscillator strength (0.1887) while that located at 6.2 eV possesses the least relative oscillator strength (0.0001).

C. Energetics of CH₃OBr and CH₃BrO. For calculation of the heats of formation of CH₃OBr at various levels of theory, an isodesmic reaction scheme, namely CH₃OBr + HOH → CH₃OH + HOBr, is employed. Isodesmic reactions are those in which the reactants and products contain the same types of bonds (i.e., the number of bonds broken and formed is conserved) and requires the heats of formation of all the molecules involved in the reaction (except that of the isomer in question) to be known. Because of this property, errors in the energy due to defects in the basis set and electron correlation cancel to a large extent. Table 4 contains values of the absolute energies for species involved in the isodesmic scheme, and Table 7 contains literature values for the heats of formation of HOH, HOBr, and CH₃OH. The results do not appear to vary much with basis set and electron correlation effects, as shown in Table 5. For CH₃OBr, the heat of formation is predicted to be -5.4 kcal mol⁻¹ at the CCSD(T)/6-311++G(3df,3pd)/B3LYP/6-311++G(3df,3pd) level of theory, which is its best estimate.

TABLE 6: Relative Energy Differences (kcal mol⁻¹)^a between CH₃OBr and CH₃BrO

levels of theory	ΔE (CH ₃ OBr - CH ₃ BrO)
B3LYP/6-311++G(3df,3pd)	41.8
B3PW86/6-311++G(3df,3pd)	40.8
B3PW91/6-311++G(3df,3pd)	40.4
B3LYP/6-311++G(3d2f,3pd)	41.6
B3PW86/6-311++G(3d2f,3pd)	40.6
B3PW91/6-311++G(3d2f,3pd)	40.1
CCSD(T)/6-311++G(3df,3pd)	42.6

^a Relative energies are corrected for zero-point energy using B3LYP/6-311++G(3df,3pd) frequencies.

TABLE 7: Heats of Formation (kcal mol⁻¹) of Species in the Isodesmic Scheme

species	$\Delta H_{f,0}^\circ$	ref
H ₂ O	-57.10 ± 0.0	<i>a</i>
HOBr	-10.93 ± 1.0	<i>b</i>
CH ₃ OH	-45.60 ± 0.1	<i>c</i>

^a Chase, M. W.; Davies, C. A.; Downey, J. R.; Frurip, D. J.; McDonald, R. A.; Syverud, A. N. *J. Phys. Chem. Ref. Data*, Suppl. 1 **1985**. ^b Ruscic, R.; Berkowitz, J. *J. Chem. Phys.* **1994**, *101*, 7795. ^c Giguere, P. A.; Liu, I. D. *J. Am. Chem. Soc.* **1955**, *77*, 6477.

The relative stability between CH₃OBr and CH₃BrO has been examined by computing the relative energy differences between them and correcting for zero-point energies, as presented in Table 6. To assess the accuracy of the relative energetic data, a calculation has been performed at the CCSD(T)/6-311++G(3df,3pd)/B3LYP/6-311++G(3df,3pd) level of theory, which generates a value of 42.6 kcal mol⁻¹. CH₃OBr appears to be lower in energy (and thus more stable) than CH₃BrO.

D. Implication for the BrO and CH₃O₂ Cross-Reaction. It has been recently postulated that the atmospheric cross-reaction between the BrO and CH₃O₂ species could play a role in stratospheric chemistry, particularly in the marine boundary layers.¹¹ For CH₃OBr to be made in the atmosphere by a

homogeneous gas-phase mechanism, the most likely pathway is the $\text{BrO} + \text{CH}_3\text{O}_2$ reaction.



There are two possible intermediates that could be formed during this reaction, namely CH_3OBr and CH_3BrO , via the channels



According to our calculations, the CH_3OBr -forming reaction channel (eq 9a) is exothermic by $-39.6 \text{ kcal mol}^{-1}$ whereas the channel for the formation of CH_3BrO (eq 9b) is endothermic by $3.0 \text{ kcal mol}^{-1}$, implying that channel 9a is thermodynamically favored.

IV. Summary

The equilibrium structures, vibrational and electronic spectra, and relative energetics of CH_3OBr and CH_3BrO have been investigated, along with the heat of formation of CH_3OBr , by the B3LYP, B3PW86, B3PW91, and CCSD(T) ab initio electronic structure methods, in conjugation with the large 6-311++G(3df,3pd) and 6-311++G(3d2f,3pd) basis sets. The CH_3OBr structural form is found to be more stable than $\text{CH}_3\text{-BrO}$. Due to its thermal stability, it is possible that CH_3OBr may play an important role in the atmospheric cross-reactions of the BrO and CH_3O_2 species.

References and Notes

(1) WMO/UNEP, *Scientific Assessment of Ozone Depletion*. Report No. 37, Geneva, Switzerland, 1994.

(2) Barrie, L. A.; Bottenheim, J. W.; Schnell, R. C.; Crutzen, P. J.; Rasmussen, R. A. *Nature* **1988**, *334*, 138.

(3) Platt, U. *Arctic Troposphere Ozone Chemistry (ARCTOC)*. Final Report to European Union, 1996.

(4) Farman, J. C.; Gardiner, B. G.; Shanklin, J. D. *Nature* **1985**, *315*, 207.

(5) Wofsy, S. C.; McElroy, M. B.; Yung, Y. L. *Geophys. Res. Lett.* **1975**, *2*, 215.

(6) Vogt, R.; Crutzen, P. J.; Sander, R. *Nature* **1996**, *383*, 327.

(7) Poulet, G.; Pirre, M.; Maguin, F.; Ramaroson, R.; Le Bras, G. *Geophys. Res. Lett.* **1992**, *19*, 2305.

(8) Larichev, M.; Maguin, F.; Le Bras, G.; Poulet, G. *J. Phys. Chem.* **1995**, *99*, 15911.

(9) Elrod, M. J.; Meads, R. F.; Lipson, J. B.; Seeley, J. V.; Molina, M. J. *J. Phys. Chem.* **1996**, *100*, 5808.

(10) Fan, S. M.; Jacob, D. J. *Nature* **1992**, *359*, 522.

(11) Aranda, A.; Le Bras, G.; La Verder, G.; Poulet, G. *Geophys. Res. Lett.* **1997**, *24* (22), 2745.

(12) Benter, T.; Feldman, C.; Kirchner, U.; Schmidt, M.; Schmidt, S.; Schindler, R. *Ber. Bunsen-Ges. Phys. Chem.* **1995**, *99*, 1144.

(13) Orlando, J. J.; Burkholder, J. B. *J. Phys. Chem.* **1995**, *99*, 1143.

(14) Helleis, F.; Crowley, J. N.; Moortgat, G. K. *Geophys. Res. Lett.* **1994**, *21*, 1795.

(15) Frisch, M. J.; Trucks, G. W.; Schlegel, H. B.; Gill, P. M. W.; Johnson, B. G.; Robb, M. A.; Cheeseman, J. R.; Keith, T.; Peterson, G. A.; Montgomery, J. A.; Raghavachari, K.; Al-Laham, M. A.; Zakrzewski, V. G.; Ortiz, J. V.; Foresman, J. B.; Cioslowski, J.; Stefanov, B. B.; Nanayakkara, A.; Challacombe, M.; Peng, C. Y.; Ayala, P. Y.; Chen, W.; Wong, M. W.; Andres, J. L.; Replogle, E. S.; Gomperts, R.; Martin, R. L.; Fox, D. J.; Binkley, J. S.; DeFrees, D. J.; Baker, J.; Stewart, J. P.; Head-Gordon, M.; Gonzales, C.; Pople, J. A. *GAUSSIAN 94, Revision D.2*; Gaussian, Inc.: Pittsburgh, PA 1995.

(16) Lee, C.; Yang, W.; Parr, R. G. *Phys. Rev. B* **1988**, *41*, 785.

(17) Perdew, J. P. *Phys. Rev. B* **1986**, *45*, 13244.

(18) Perdew, J. P.; Wong, Y. *Phys. Rev. B* **1992**, *45*, 13244.

(19) Foresman, J. B.; Head-Gordon, M.; Pople, J. A.; Frisch, M. J. *J. Phys. Chem.* **1992**, *96*, 135.

(20) Lee, T. J.; Rendell, A. P. *J. Chem. Phys.* **1991**, *94*, 6219.

(21) Lee, T. J. *J. Phys. Chem.* **1995**, *99*, 15074.

(22) Venkateswartha, P.; Gordy, W. *J. Chem. Phys.* **1955**, *23*, 1200.

(23) Francisco, J. S.; Hand, M. R.; Williams, I. H. *J. Phys. Chem.* **1996**, *100*, 9250.

(24) Tanaka, C.; Kuratani, K.; Mizushima, S. *Spectrochim. Acta* **1957**, *9*, 265.

(25) Thiel, M. V.; Becker, E. D.; Pimentel, G. C. *J. Chem. Phys.* **1957**, *27*, 95.